Iodosylbenzene Coordination Chemistry Relevant to MOF Catalysis

Ashley D. Cardenal,† Asim Maity,† Wen-Yang Gao, Rahym Ashirov, Sung-Min Hyun, David C. Powers*

Department of Chemistry, Texas A&M University, College Station, Texas 77843, United States

Supporting Information Placeholder

ABSTRACT: Hypervalent iodine compounds formally feature expanded valence shells at iodine. These reagents are broadly used in synthetic chemistry due to the ability to participate in well-defined oxidation-reduction processes and because the ligand-exchange chemistry intrinsic to the hypervalent center allows hypervalent iodine compounds to be applied to a broad array of oxidative substrate functionalization reactions. We have recently developed methods to generate these compounds from O_2 that are predicated on diverting reactive intermediates of aldehyde autoxidation towards the oxidation of aryl iodides. Coupling the aerobic oxidation of aryliodides with catalysts that effect C–H bond oxidation would provide a strategy to achieve aerobic C–H oxidation chemistry. In this Forum article we discuss the aspects of hypervalent iodine chemistry and bonding that render this class of reagents attractive lynchpins for aerobic oxidation chemistry. We then discuss the oxidation processes relevant to the aerobic preparation of 2-(*tert*-butylsulfonyl)iodosylbenzene, which is a popular hypervalent iodine reagent for use with porous metal-organic framework-based catalysts because it displays significantly enhanced solubility as compared with unsubstituted iodosylbenzene. We demonstrate that popular synthetic methods to this reagent often provide material that displays unpredictable disproportionation behavior due to the presence of trace impurities. We provide a revised synthetic route that avoids impurities common in the reported methods and provides access to material that displays predictable stability. Finally, we describe the coordination chemistry of hypervalent iodine compounds with metal clusters relevant to MOF chemistry and discuss the potential implications of this coordination chemistry to catalysis in MOF scaffolds.

Introduction

Background and History. Iodine was discovered in 1811 by Bernard Courtois and was named by Joseph Louis Gay-Lussac in 1813 (the name "iodine" derives from the Greek word ἰώδης, which means "violet colored").[1] The chemistry of iodine, which is the largest, least electronegative, and most ionizable of the non-radioactive halogens,[2] is dominated by the (0) and (−1) oxidation states (*i.e.* I_2 and I^-). Facile interconversion of I(0) and I(−1) by oxidation-reduction chemistry underpins the I^- / I_3^- redox couple that is critical to the chemistry of dye-sensitized solar cells.[3] The ionizability of iodine is manifest in a rich body of iodine-centered redox chemistry and the availability of families of compounds featuring iodine in oxidation states greater than zero (Figure 1). For example, exposure of I_2 to SbF_5 results in the formation of the $[I_2^+]$-containing salt $[I_2][Sb_2F_{11}]$ (Figure 1a).[4-5] Dimerization of I_2^+ to afford I_4^{2+} has been observed,[6-7] and higher-order iodine cations, such as I_3^+, I_5^+, I_7^+, and I_{15}^+ have been characterized.[6] Higher oxidation state iodine species are also commonly encountered in iodine oxyacids of I(I), I(III), I(V), and I(VII) (*i.e.* HIO, HIO_2, HIO_3, and HIO_4), iodine oxides, and iodine fluoride (*i.e.* IF_7) (Figure 1b).

Higher oxidation states of iodine are also encountered in organoiodine chemistry (Figure 1c). In 1886, Willgerodt reported the preparation of $PhICl_2$, which features an I(III) center, upon passage of Cl_2 through a solution containing PhI.[8] Since this original discovery, an enormous array of I(III) derivatives have been prepared.[9] $PhICl_2$ is a T-shaped molecule and formally features a dectet electronic configuration at iodine. As such, these compounds are termed hypervalent, which Musher defined as: "atomic centers which exceed the number of valences allowed by the traditional theory, and thus utilize more electron-bonding pairs than provide stability in the Lewis Langmuir theory."[10] Various nomenclature schemes have been utilized to describe hypervalent I(III) compounds. According to IUPAC convention for compounds with non-standard coordination numbers, organic compounds containing I(III) centers are referred to as λ^3-iodanes.[11] Martin-Arduengo N–X–L nomenclature, in which *N* is the number of valence electrons formally assigned to iodine, *X* is the identity of the hypervalent element,

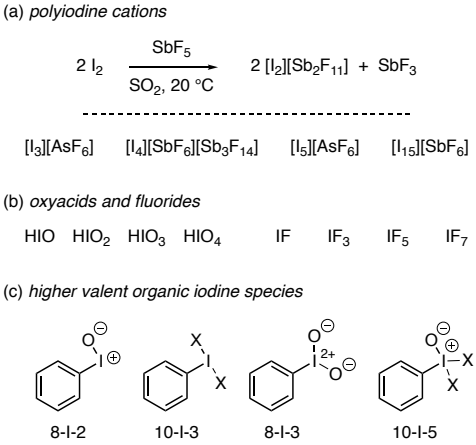

Figure 1. The low ionization potential of iodine is manifest in families of oxidized iodine compounds. Examples include (a) polyiodine cations, (b) iodine oxyacids and fluorides, and (c) λ^3- and λ^5-iodanes.

and *L* is the number of ligands attached to the hypervalent atom, is also frequently used to describe higher valent organoiodides.[12-13] In addition, a large array of I(V)-containing compounds (*i.e.* Dess-Martin periodinane and IBX; λ^5-iodanes), which feature a dodectet electronic configuration at iodine, have been prepared.[14-19] There are no examples of organic I(VII)-containing compounds.

Historically, bonding models based on either 1) participation of vacant iodine-centered d-orbitals in hybridization, or 2) bonds with greater than 50% ionic character, which would result in localization of electron density on ligand-borne orbitals, have been advanced to rationalize the apparent valence expansion at iodine in λ^3- and λ^5-iodanes.[20] In 1951, Rundle and Pimentel advanced the now-accepted model for hypervalent iodine bonding based on overlap of the 5p orbital at iodine with ligand-centered orbitals to give rise to the electron-rich 3c-4e bonding picture illustrated in Figure 2.[21-22] Population of bond ψ_1 and non-bonding ψ_2 gives rise to the observed linear L–I–L triads. Violation of the octet at iodine is avoided by localization of two electrons in ligand-borne ψ_2. In addition to avoiding violation of the octet rule, this picture rationalizes the observation of highly ionic bonding in hypervalent iodine compounds and the preference for electronegative substituents to occupy the hypervalent bond. Further experimental support for the ionic bonding in hypervalent iodine molecules is the observation that the iodine center can serve as an acceptor in halogen bonding interactions.[23-24] Due to population of both bonding and non-bonding orbitals, the I–L bond lengths in hypervalent iodine species are typically intermediate between the sum of the covalent and ionic radii of the relevant atoms.[25] The bonding picture of I(V) derivatives mirrors that of I(III) compounds except that there are two (orthogonal) hypervalent 3c-4e bonds.

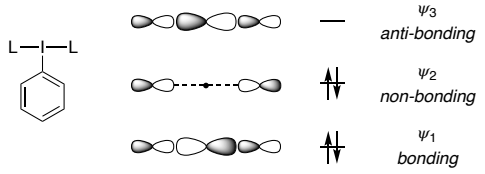

Figure 2. Orbital picture for the 3c-4e bonding in hypervalent iodine compounds. Population of ψ_2, which is ligand centered, allows accommodation of the formal octet violations at iodine without utilizing d-orbital hybridization. In neutral I(III) derivatives, L represents an anionic donor ligand.

Iodosylbenzene derivatives (*i.e.* 8-I-2 species) also feature I(III) centers. While these species are often drawn with I–L multiple bonds (*i.e.* PhI=O), the large radius of iodine results in insignificant π-bonding.[26] Poor π overlap results in highly polarized bonding, (*i.e.* $PhI^+–O^-$). The extensive polarization of the I–O bond often results in solid-state –I–O–I–O– polymerization driven by charge pairing,[27-29] which results in poorly soluble materials. Iodosylbenzenes are metastable with respect to disproportionation to I(I) and I(V) species, although sufficiently large kinetic barriers to disproportionation often allow for straightforward handling of I(III) species. For example, the disproportionation of $(PhIO)_n$ to generate iodobenzene and iodylbenzene is spontaneous,[30] but requires either catalysts (*i.e.* $RuCl_3$[31]) or elevated temperatures[32] to proceed at appreciable rates. The mechanism of disproportionation has not been extensively investigated but has been suggested to proceed via oxygen-atom transfer chemistry in an *O*-bridged diiodine intermediate.[33] As a result of the aforementioned disproportionation thermodynamics, iodylbenzenes are weaker oxidants than iodosylbenzenes.

The reaction chemistry of hypervalent iodine compounds resembles that of the more toxic main-group analogues based on Hg(II), Tl(III), and Pb(IV)[15] and is frequently described using terminology common to organometallic mechanisms.[34] The oxidation of PhI to $PhICl_2$ described above represents an oxidative addition reaction at the iodine center (Figure 3a).[8] Ligand exchange chemistry is often facile at iodine; for example, the alkoxide ligand exchange at iodine pictured in Figure 3b is rapid at room temperature.[35] Both associative and dissociative exchange mechanisms have been proposed.[36] Reductive elimination, in which ligand coupling from the hypervalent iodine center is accomplished with concurrent formation of an aryl iodide are ubiquitous (Figure 3c). Both inner-sphere ligand coupling and outer-sphere, nucleophilic aromatic substitution pathways have been suggested for the observed elimination reactions.[37-38] Reductive elimination processes are driven by the hypernucleofugacity of PhI. Finally, group-transfer chemistry of iodosylbenzenes, for example in the synthesis of metal oxo complexes[37, 39-40] as well as in hydroxylation catalysisis, is very frequently encountered (Figure 3d).[41-42] The importance of hypervalent iodine compounds has resulted in an extensive review literature of the chemistry and reactivity of these compounds.[15-16, 18-19, 43-45] Similar to the oxidation-reduction cycling that underpins hypervalent iodine catalysis, oxidation-reduction cycling with other main-group elements, such as phosphorous, has recently emerged as an opportunity in metal-free catalysis.[46-49]

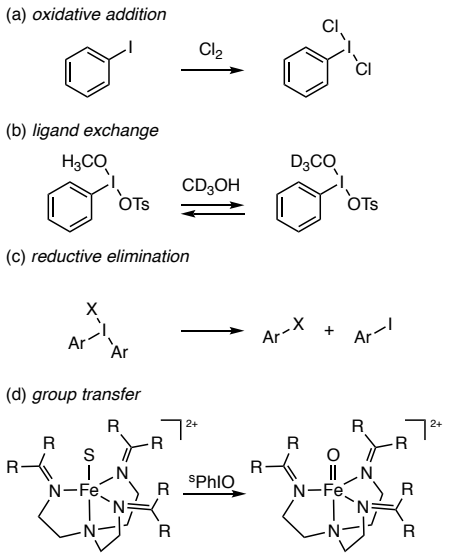

Figure 3. The chemistry of hypervalent iodine compounds is often described using terminology common to organometallic catalysis because hypervalent iodine compounds participate in (a) two-electron iodine-centered oxidation, (b) ligand exchange chemistry, (c) reductive elimination reactions, and (d) group-transfer processes. R = $N(CH_3)_3$; S = CH_3CN; ^{s}PhIO = 2-(*tert*-butylsulfonyl)iodosylbenzene (**1**).

Interest in hypervalent iodine chemistry has, in large part, been motivated by the utility of these reagents as non-toxic, selective oxidants in synthetic chemistry. Iodosylbenzene derivatives have been applied to α-oxidation of carbonyls,[50] oxidative 1,2-difunctionalization of olefins,[51] oxidative dearomatization chemistry,[52-55] cross-coupling reactions,[56-57] and have found important application as group-transfer reagents in organometallic catalysis.[18, 58] The facility of ligand exchange at hypervalent iodine centers underpins the breadth of substrate functionalization chemistry that can be achieved with hypervalent iodine compound: In addition to oxygen transfer, halogen, nitrogen, and hydrocarbyl transfer reactions are all common. I(V) reagents display complementary substrate functionalization chemistry, most notably towards alcohol and amine dehydrogenation reactions.[14-19]

Towards Hypervalent Iodine Mediated Aerobic Hydrocarbon Oxidation. The proclivity of iodosylbenzene derivatives to participate in group-transfer chemistry has stimulated substantial interest in using these reagents as terminal oxidants in oxidation catalysis. Motivated by 1) the potential to utilize metal-organic frameworks (MOFs) to prevent bimolecular decomposition chemistry by site-isolating catalyst sites and 2) the potential to leverage network porosity as an opportunity to non-covalently co-localize substrate in proximity of reactive intermediates,[59] iodosylbenzenes have found widespread application as terminal oxidants in MOF catalysis: The facility with which ligand exchange proceeds at the hypervalent iodine center has enabled both C–H oxygenation[60-62] and C–H amination[63] reactions using MOF catalysts. The solubility of hypervalent iodine reagents is critical to proposals of substrate functionalization in the interstices of porous materials. In this context, 2-(*tert*-butylsulfonyl)iodosylbenzene (**1**),[60-62, 64] in which secondary bonding between the hypervalent iodine center and the proximal Lewis base promotes iodosylbenzene depolymerization and solubilization of monomeric species,[65] has emerged as an important terminal oxidant in MOF catalysis.

We have been motivated by the potential to develop aerobic hydrocarbon functionalization chemistry by coupling the aerobic generation of hypervalent iodine reagents with appropriate catalysts. In 2018, we reported the aerobic synthesis of hypervalent iodine compounds based on intercepting reactive oxidants generated during aldehyde autoxidation with aryl iodides.[66] In concept, the development of aerobic synthetic approaches to hypervalent iodine species contributes to sustainable synthetic chemistry by avoiding the metal-based oxidants that are often encountered in hypervalent iodine chemistry. To the extent that the developed aerobic oxidation methods can be coupled with iodine catalysis, the methods also contribute to relieving the requirement for (super)stoichiometric loading of hypervalent iodine reagents. Initial efforts to aerobically generate soluble iodosylarene **1** failed to provide access to I(III) species, and instead afforded iodylarene **2**. The aforementioned disproportionation thermodynamics of I(III) species imply that I(V) reagents are less strongly oxidizing than the related I(III) derivatives. The differing oxidation behaviors of **1** and **2** are manifest in the Mn(salen) catalyzed epoxidation of styrene (Figure 4). In the original report of the synthesis of **1**, Protasiewicz and co-workers showed that **1** is an effective terminal oxidant for this transformation,[67] and this report has been reproduced in our laboratory. In contrast, replacement of I(III) reagent **1** with I(V) reagent **2** results in the observation of no epoxidation.

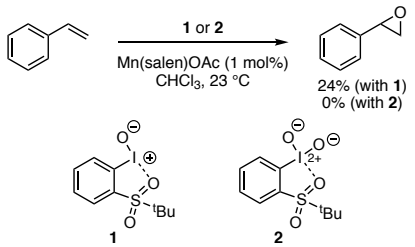

Figure 4. The oxidation of styrene to styrene oxide proceeds from iodosylarene **1** but does not proceed with iodylarene **2**.

In order to rationally advance our goals of aerobic oxidation catalysis, we are critically interested in understanding the disproportionation behavior of soluble iodosylbenzenes in greater detail and in understanding potential interactions of those iodosylbenzene reagents with the transition metal nodes that comprise critical structural units in MOFs. We originally proposed that disproportionation of initially formed I(III) species was promoted by AcOH, which is an obligate by-product of acetaldehyde-promoted aerobic oxidation chemistry. Continued investigations have suggested that AcOH-promoted disproportionation is not a viable pathway for synthesis of **2** (*vide infra*). Here we describe preparation-dependent behavior of reagent **1** and show that popular methods to prepare this reagent can provide access to material that displays unpredictable disproportionation rates. In addition, we examine the chemistry of iodosylarenes with soluble models of the transition metal clusters common to Zr_6- and Zn_2-based MOFs and show that both ligand-exchange reactions as well as the formation of acid-base adducts are available. These observations may provide insight into potential interactions between iodosylarenes and structural nodes common to metal-organic framework catalysts.

Results and Discussion

*Structure and Bonding of 2-(*tert*-Butylsulfonyl)iodosylbenzene* (**1**). Consistent with the analysis of a hypothetical monomeric PhIO by Zhdankin and Boldyrev and co-workers,[25] natural bond order (NBO) analysis indicates the lack of meaningful I–O π-bonding in **1**. In addition to the I–O σ bond, the valence at oxygen is completed with three non-bonding electron pairs (Figure 5; coordinates of computed structures collected in Tables S1–S2). The calculated Wiberg I–O bond order is 1.05 and analysis of the natural charges of iodine (+1.33) and oxygen (–1.06) is consistent with highly ionic I–O bonding. Comparison of the computational results for **1** with those for a hypothetical monomeric PhIO unit indicates the natural charge of the iodosyl oxygen atom is slightly more negative in **1** than in PhIO (–1.06 *vs.* –1.01), which is consistent with the presence of a *trans*-influencing sulfonyl ligand at iodine.[25, 68]

The highly polarized I–O bond in **1** manifests in oxygen-centered Lewis basicity, which is evidenced by a hydrogen-bonded chloroform molecule in the original crystal structure of this molecule (distance between H-bond donor and

accepter is 3.046 Å).[67] Examination of the ^{1}H NMR spectrum of **1** in the presence of hexafluoroisopropanol (HFIP), which is frequently employed as a solvent or additive in iodine-mediated group-transfer catalysis,[69-74] revealed [HFIP]-dependent chemical shifts (Figure S1). Crystallization of **1** in the presence of excess HFIP resulted in the isolation of **1**·HFIP in which the HFIP molecule is H-bonded to the iodosylbenzene oxygen (Figure 6, X-ray data tabulated in Table S6). The distance between H-bond donor and accepter in **1**·HFIP is 2.586 Å. The relative shortness of the H-boning in **1**·HFIP versus between **1** and chloroform is consistent with the relative acidities of HFIP and $CHCl_3$ (pKa = 9.3 and 15.5, respectively). Upon binding to HFIP, the I–O bond (I(1)–O(1)) elongates from 1.848(6) to 1.873(4) Å and the I–O distance to the sulfonyl oxygen (I(1)–O(2)) contracts from 2.707(5) to 2.668(3) Å (Figure 6).[75] NBO analysis of **1**·HFIP resulted in natural charges for iodine and oxygen of +1.38 and −1.06, respectively, which indicates enhancement of positive charge at iodine upon HFIP binding. A combination of COSY, HSQC, and HMBC NMR experiments enabled unambiguous assignment of the proton resonances of both **1** and **1**·HFIP (Figures S2-S7 and Tables S4 and S5). Analysis of the $\Delta\delta$ ^{1}H resonance of the C–H *para* to iodine vs. [HFIP] enabled the equilibrium constant to be determined (K_{eq} = 0.037 ± 0.004), which corresponds to ΔG = 1.94 ± 0.06 kcal/mol

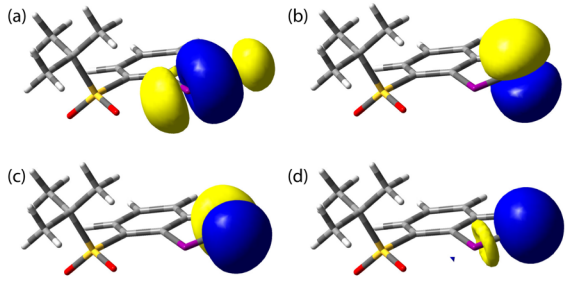

Figure 5. NBO orbitals for **1** that show (a) I–O σ-bonding and (b–d) O-centered lone pairs.

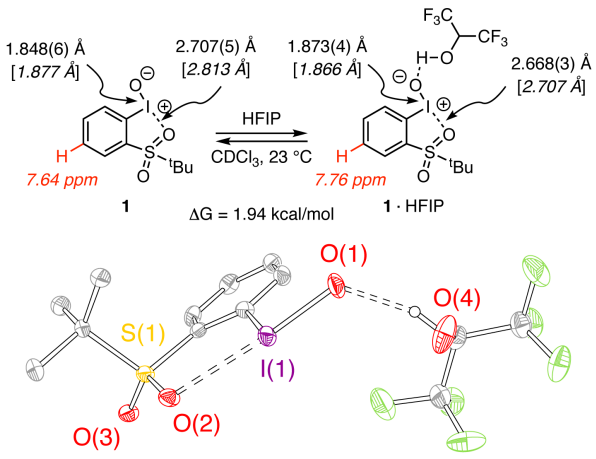

Figure 6. Top: Addition of HFIP to iodosyarene **1** results in the formation of H-bonded adduct **1**·HFIP. The thermodynamics of HFIP binding have been examined by analyzing the perturbation of the chemical shift of proton *para* to iodine as a function of [HFIP]. Bottom: Solid-state structure of **1**·HFIP, which shows that the iodosyl I–O bond (I(1)–O(1)) elongates and the contact between hypervalent iodine center and the sulfonyl group (I(1)–O(2)) contracts upon binding with HFIP.

(Figure 6). While HFIP is regularly used as a solvent or additive in hypervalent iodine chemistry, the role of adducts such as **1**·HFIP is not clear based on the data we have collected: for example, use of **1**·HFIP in the styrene epoxidation illustrated in Figure 4 results in similar styrene oxide yields as when **1** is used as the terminal oxidant.

In contrast to the adduct formation observed between **1** and HFIP, exposure of iodosylbenzene ($(PhIO)_n$) to HFIP results in complete dissolution of the solid $(PhIO)_n$ polymer and formation of $PhI(OC(H)(CF_3)_2)_2$ (Eqn. 1). Formation of the *bis*-alkoxide adduct is evidenced by the appearance of a methine resonance at 4.20 ppm that integrates for two protons (Figure S8). Similar to the formation of **4**, Hill *et al.* reported that $(PhIO)_n$ dissolves in CH_3OH to afford $PhI(OCH_3)_2$.[76] Compound **4** is unstable towards isolation, which is consistent with previous reports of fluoroalkoxide adducts of iodosylbenzenes that have been generated electrochemically.[77-79]

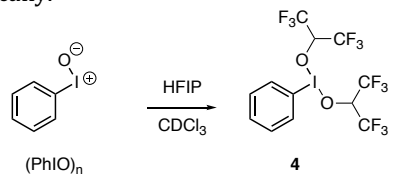

(1)

*On the Aldehyde-Promoted Aerobic Oxidation of 2-(*tert*-Butylsulfony)liodobenzene (**3**).* In our original report of the aerobic oxidation of 2-(*tert*-butylsulfonyl)iodobenzene (**3**), we demonstrated that our aldehyde-promoted aerobic oxidation conditions provide direct access to I(V) derivative **2** (Figure 7a).[80] We proposed that the observation of I(V) was due to AcOH-promoted disproportionation of an initially formed iodosylbenzene intermediate based on the following observations: 1) *in situ* monitoring of the oxidation of iodoarene **3** revealed that **3** and I(V) compound **2** were the only observable iodine-containing species and that I(III) compound **1** (or *bis*-acetate adduct **5**) was not present in the reaction mixture; and 2) disproportionation of independently synthesized iodosylarene **1** to generate equimolar amount of I(I) and I(V) was observed upon addition of AcOH. The proposed acid-promoted disproportionation was consistent with literature detailing O-bridged intermediates in disproportionation reactions in acidic media.[33, 81-82] *During subsequent investigations of the reaction chemistry of **1** with AcOH, we have observed that in contrast to the observed disproportionation, diacetate **5** formed in the presence of AcOH and this species appears to be resistant to disproportionation (Figure 7b and S9).* To clarify the divergent results regarding the disproportionation of **1**, we have pursued the following series of experiments.

*Synthesis of Iodosylarene **1**.* A variety of procedures have been reported for the synthesis of **1** (Methods A–C, Eqn. 2). In the original report from Protasiewicz, aryl iodide **1** was treated with H_2O_2 in Ac_2O and then 3M NaOH to generate **1** (Method A).[67] Concerns regarding the safety of this procedure have been raised,[83] and as a result, methods based on oxidation with either $KClO_3$ in HCl or $NaBO_3$ in AcOH followed by hydrolysis with NaOH have been developed.[62, 84] In our hands, Method B, based on treatment of **3** with $KClO_3$ and HCl, provided an analytically pure sample of **1** (assayed by combustion analysis). Despite the apparent purity of the samples obtained by this method, we found that samples of **1** prepared by Method B exhibit substantial variation with

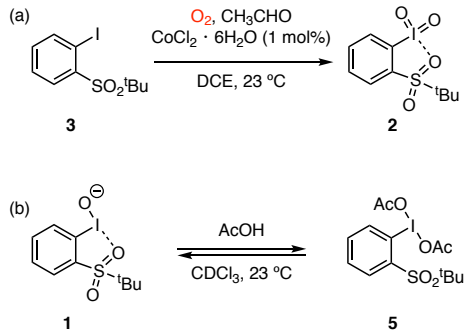

Figure 7. (a) Aldehyde-promoted aerobic oxidation of 2-(*tert*-butylsulfonyl)iodobenzene (**3**) affords iodylarene **2**. Iodosylarene **1** is not observed at intermediate reaction times. (b) Exposure of iodosylarene **1** to AcOH, which is an obligate by-product of the autoxidation of acetaldehyde, affords *bis*-acetate **5**.

respect to disproportionation rate: In a series of ^{1}H NMR experiments using mesitylene as an internal standard, half-lives ranging from less than a minute to six hours have been observed. In addition, the material appeared to be light sensitive, showing accelerated disproportionation when exposed to ambient light.

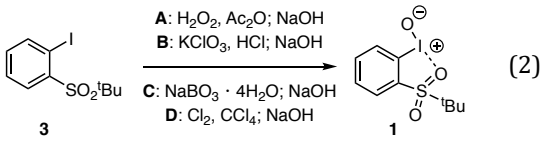

(2)

We speculated that the unpredictable disproportionation rates displayed by samples of **1** prepared by Method B may be due to the presence of a trace impurity in the reagent that is not detected by combustion analysis. To evaluate the potential presence of impurities in the samples of **1**, we have pursued EPR and mass spectrometry-based experiments. Exposure of a sample of **1** prepared by Method B to *N*-*tert*-butyl-α-phenylnitrone (PBN), which is a commonly used EPR spin trap,[85] in $CDCl_3$ results in the EPR spectrum shown in Figure 8a (see also Figure S10), which can be fit as the admixture of the spectrum of oxidized PBN as well as the spectrum of the PBN adduct of hydroxy radical (Figure 8b). The intensity of the spectral features increases upon exposure of the sample to ambient light (Figure S11). An identical EPR spectrum can be obtained from $KClO_3$ in $CDCl_3$ (Figure S12). These observations are consistent with the presence of a trace quantity of chlorate that was not removed despite extensive washing; UV irradiation of chlorate has been reported to promote a variety of radical-generating processes.[86] Dissolution of the sample of **1** prepared by Method B in HNO_3 and analysis by ICP-MS indicated the presence of K^+. Chlorate is not detectable by IR analysis (Figure S13), however, negative-mode ESI-MS of **1** prepared by Method **B** indicates the presence of ClO_3^- (*m/z* = 82.953 (expt); 82.954 (calc)) (Figure S14). We suspect that the source of the observed potassium is the $KClO_3$ used to prepare **1**.

Based on the hypothesis that trace impurities associated with $KClO_3$ were leading to the irreproducible disproportionation behavior of **1**, we modified the synthetic protocol

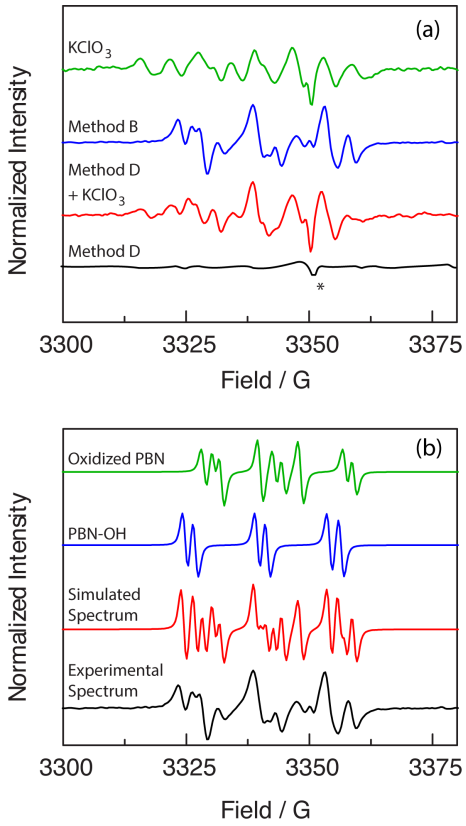

Figure 8. (a) EPR spectra obtained following PBN addition to **1** prepared by Method D (—), **1** with added $KClO_3$ (—), **1** prepared by Method B (—), and $KClO_3$ (—); * this signal is from the resonator background. (b) Simulated EPR components: Experimentally obtained spectrum following PBN addition to **1** prepared by Method D with added $KClO_3$ (—), spectral simulation as admixture of oxidized PBN and hydroxy radical adduct (—), simulated PBN-adduct of hydroxyl radical (—), and simulated spectrum for oxidized PBN (—).

as follows: Cl_2 was bubbled through a solution of **3** in CCl_4, the resulting solid was isolated, and was then treated with 5M NaOH solution (Method D, Eqn 2). The resulting samples of **1** display reproducible disproportionation chemistry (*vide infra*). Exposure of material prepared by Method D to PBN did not give rise to an observable EPR signal (Figure 8a and Figure S15). Addition of $KClO_3$ to the sample of **1** prepared from Method D led to the evolution of an EPR spectrum (Figure S16) that overlays the spectrum obtained from Method B (Figure 8a) and the intensity of the signal increased upon exposure to light (Figure S17). In addition, ICP-MS analysis of **1** prepared by Method D did not show the presence of any trace metal ions.

With access to samples of **1** obtained from Method D, we have investigated the kinetics of reagent disproportionation. Disproportionation was monitored by ^{1}H NMR spectroscopy utilizing mesitylene as an internal standard. Monitoring the concentration of **1** as a function of time at 48 °C revealed that disproportionation is second-order with respect to **1** (Figure 9 and Figure S18). Examination of the disproportionation as a function of temperature from 35–75 °C allowed construction of the Eyring plot shown in Figure 9b

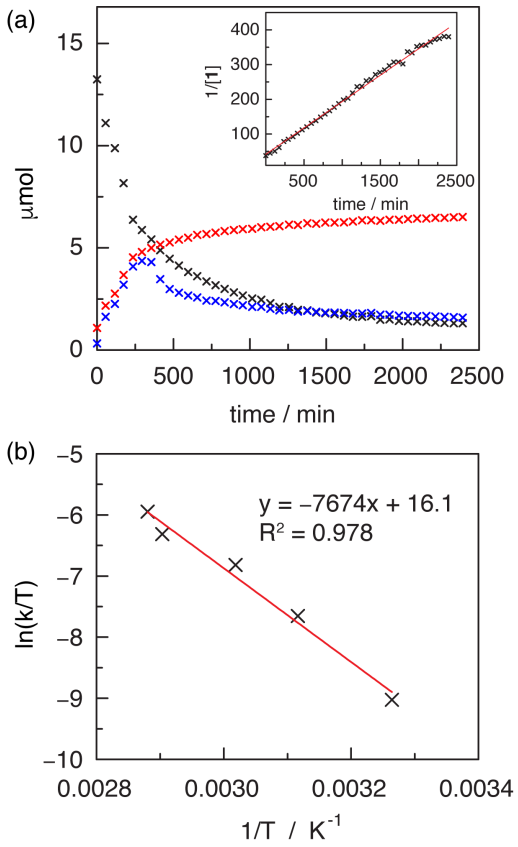

Figure 9. (a) Concentration vs. time plot of 2-(*tert*-butylsulfonyl)iodosylbenzene (**1**, ×), 2-(*tert*-butylsulfonyl)iodobenzene (**3**, ×), and 2-(*tert*-butylsulfonyl)iodylbenzene (**2**, ×) for the disproportionation of **1** at 48 °C in $CDCl_3$. At ~300 minutes, precipitation of **2** was observed which accounts for the observed decreasing concentration at this time. Inset: Plot of $[\mathbf{1}]^{-1}$ vs. time for the disproportionation of **1** at 48 °C in $CDCl_3$. (b) Eyring plot for the disproportionation of **1**.

(also see, Figure S19-S23). From these data, activation parameters for disproportionation — $\Delta H^{\ddagger}$ = 15.2 kcal·mol^{-1} and $\Delta S^{\ddagger}$ = –15.2 cal·K^{-1}mol^{-1} — can be extracted (Figure S24). High-resolution positive-mode ESI-MS analysis of disproportionation reaction mixtures indicates the presence of dimeric species (*i.e. m/z* = 680.9294, calc for $[\mathbf{1}]_2H^+$ = 680.9333; (Figure S25). In combination with the observed second order kinetics, these data suggest that disproportionation of **1** proceeds by oxygen-atom transfer via *O*-bridged dimeric intermediates, which is consistent with previous mechanistic proposal for iodosylbenzene disproportionation.[33, 81-82]

Regarding the formation of iodylarene **2** by aldehyde-promoted aerobic oxidation, the above experimental data suggest that our original proposal of acid-promoted disproportionation of **1** was based on the irreproducible disproportionation kinetics of material prepared by Method B. While a detailed understanding of the mechanism of aerobic production of iodylarene **2** during aldehyde-promoted aerobic oxidation is beyond the scope of our current work, we note the following relevant observations (summarized in Figure S26):

(1) While the oxidation of 4-iodotoluene to the corresponding iodylbenzene under the action of O_2, CH_3CHO, and Co(II) proceeds via the initial formation of 4-iodotoluene diacetate (*i.e.* I(III)) followed by subsequent oxidation of I(III) to I(V), oxidation of iodoarene **3** affords iodylarene **2** without the observation of iodosylarene **1** or *bis*-acetate **5**.[80]

(2) Addition of the isolable reaction components of aldehyde-promoted aerobic oxidation, including acetaldehyde (Figure S27), acetic acid, $CoCl_2$ (Figure S28), and $Co(OAc)_3$ (Figure S29), does not induce disproportionation of *bis*-acetate **5**.

(3) Exposure of an independently prepared sample of I(III) compound **5** to aldehyde-promoted aerobic oxidation (O_2, CH_3CHO, and Co(II) in d_4-AcOH) resulted in the observation of both iodylarene **2** and iodoarene **3** by ^{1}H NMR (Figure S30). The presence of iodoarene **3** during the aerobic oxidation of **5** suggests that a disproportionation mechanism may be operative.

(4) Monitoring the oxidation of iodoarene **3** with commercially available 32 wt% peracetic acid by ^{1}H NMR revealed 1) two-phase kinetic behavior and 2) initial buildup and subsequent consumption of *bis*-acetate **5** (Figure S31). The two-phase kinetics during the oxidation of iodoarene **3** was observed due to the presence of H_2O_2 in commercially available peracetic acid solutions. During this kinetic phase, H_2O_2 reduces the I(III) (*i.e.* either **1** or **5**) formed by peracetic acid to regenerate iodoarene **3** and $^1O_2$ (observed as small bubbles).[80] Generation of $^1O_2$ was confirmed by the observation of 9,10-dimethyl-9,10-dihydro-9,10-epidioxyanthracene upon addition of 9,10-dimethylanthracene, a common chemical trap for $^1O_2$ (Figure S32). Independent reaction of either **1** or **2** with H_2O_2 resulted in iodine-centered reduction and evolution of $^1O_2$ (Figures S33 and S34, respectively). After the initial kinetic phase, accumulation of **5** was observed which is then further oxidized to iodylarene **2**. Similar generation and trapping of $^1O_2$ during reaction of H_2O_2 with $Ph(I(O_2CF_3)_2$ has previously been observed.[87-88]

Coordination Chemistry of Iodosylbenzenes with Soluble Transition Metal Clusters. Hypervalent iodine compounds have found important applications in MOF catalysis:[89] Compound **1** has been applied in MOF-catalyzed epoxidation,[61-62, 64, 90] hydroxylation,[60] and amination reactions.[63] Following the observation of the disparate coordination chemistry of **1** and $(PhIO)_n$ with HFIP, we have undertaken an examination of the potential coordination chemistry of these iodosylbenzenes with transition metal clusters that are commonly encountered in MOF chemistry. We selected a carboxylate-bridged Zn_2 complex (**6**)[91] and a Zr_6O_4 cluster (**7**)[92-93] as exemplary models because 1) these coordination sites are ubiquitous in MOF chemistry,[94] and 2) the ligand exchange rates of Zn and Zr are drastically different,[95] and thus these complexes provide a probe for the impact of M–L bond lability on the interaction of the cluster with iodosylbenzenes.

Exposure of both Zn_2 and Zr_6 clusters to $(PhIO)_n$ resulted in $(PhIO)_n$ dissolution and the observation of the $PhI(OR)_2$ species derived from carboxylate exchange; iodobenzene dibenzoate is observed following treatment of Zn_2 complex **6** with $(PhIO)_n$ and iodobenzene dimethacrylate is obtained following treatment of Zr_6 cluster **7** with $(PhIO)_n$ (Figure 10, Figures S35 and S36). In neither case have we characterized

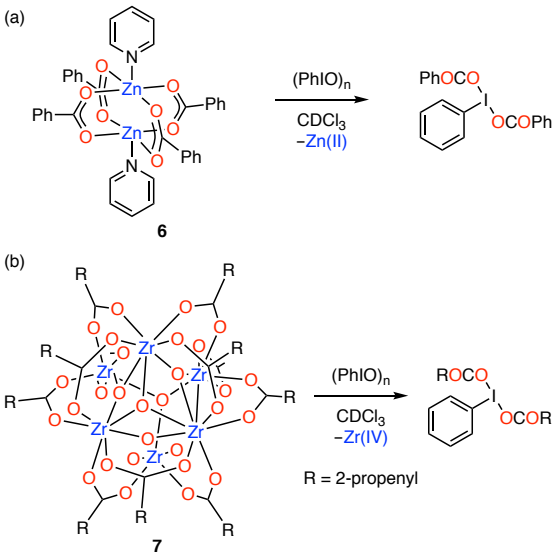

Figure 10. Ligand exchange is observed between $(PhIO)_n$ and (a) Zn_2 complex **6** and (b) Zr_6 cluster **7**.

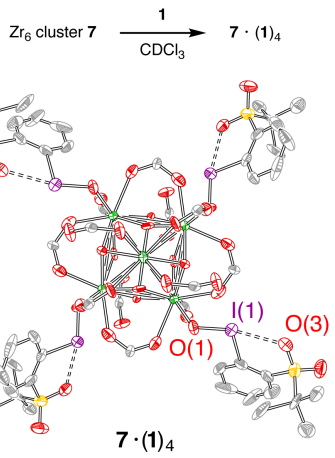

Figure 11. Exposure of Zr_6 cluster **7** to iodosylarene **1** results in isolation of **7**·(**1**)$_4$; I(1)–O(1) = 1.87(1) Å and I(1)–O(3) = 2.62(2) Å.

the metal-containing byproducts of these exchange reactions.

In contrast to the ligand exchange chemistry observed between $(PhIO)_n$ and complexes **6** and **7**, iodosylarene **1** does not participate in analogous ligand exchange chemistry. Exposure of **1** to Zn_2 benzoate complex **6** does not result in the observation of benzoate adducts of **1**, which would arise by carboxylate exchange similar to that observed for reaction of $(PhIO)_n$ with **6** (Figure S37). Treatment of Zr_6 cluster **7** with excess iodosylarene **1**, such as would be present during catalysis, results in the isolation of a new Zr_6 cluster **7**·(**1**)$_4$, in which four molecules of **1** are bound to the Zr_6 core (Figure 11, Figure S38). Upon binding, the coordination mode of the carboxylates changes; whereas in the starting Zr_6 cluster nine carboxylate ligands engage in bridging binding modes and three chelate to a single Zr center, in cluster **7**·(**1**)$_4$ eight carboxylates participate in bridging binding modes and four are monodentate. These observations indicate that ligation of iodosylbenzene to Zr is capable of displacing both bridging and chelating carboxylate ligands. Analysis of the metrical parameters of the iodosylbenzene fragments bound to Zr indicates that the I–O bond elongates from 1.848(6) to 1.87(1) Å and the secondary bonding interaction between the sulfonyl oxygen and the iodine center contracts from 2.707(5) to 2.62(2) Å. The perturbations are similar to those observed to result from HFIP binding to **1** in **1**·HFIP. Similarly, I–O bond elongation and contraction of secondary bonding interactions have consistently been observed in the limited number of previously reported transition metal adducts of iodosylarene **1** (metrical parameters of transition metal adducts of **1** are compared in Table S6).[30, 96-100] We speculate that the disparate behaviors of $(PhIO)_n$ and **1** towards ligand exchange and Lewis adduct formation, respectively, is due to the secondary coordination in **1**, which amplifies the basicity of the iodosyl oxygen.

Investigation of Potential Coordination Chemistry in MOFs. Based on the observation of ligand exchange processes (with $(PhIO)_n$) and ligand displacement reactions (with iodosylarene **1**) between iodosylarenes and transition metal clusters, we have pursued a preliminary investigation of the potential for similar coordination chemistry to impact the structure of MOFs comprised of these building units. To this end, we have examined the chemistry of UiO-67,[101] which is comprised of Zr_6 nodes, and MOF-508,[102-103] which is based on Zn_2 nodes. These materials were selected because they lack redox-active metal sites, which would complicate analysis by providing pathways for iodosylarene redox chemistry. Incubation of these materials with either **1** or $(PhIO)_n$ does not result in the observation of changes to the PXRD patterns (Figures S39–S42) or the observation of linker-derived soluble species by ^{1}H NMR. These observations suggest that the reaction chemistry observed with soluble Zn_2 and Zr_6 clusters is less important in extended materials, which is likely due to effective stabilization of M–L bonds by a macromolecular chelate effect.

Conclusions

Hypervalent iodine compounds featuring I(III) and I(V) centers are accessible due to high ionizability of iodine. Due to the importance of 3c-4e bonds, the I–L bonds in hypervalent iodine compounds are highly ionic. The facility of oxidation-reduction chemistry at iodine coupled with the ligand exchange chemistry that is characteristic of hypervalent iodine compounds gives rise to reactivity patterns that bear similarity to the reaction chemistry of transition metal complexes. Recently, 2-(*tert*-butylsulfonyl)iodosylbenzene (**1**) has garnered substantial attention from the MOF catalysis community because it exhibits substantially greater solubility in organic solvents than does $(PhIO)_n$, which is critical to achieving interstitial MOF catalysis. We have been attracted to the challenge of developing aerobic methods to generate soluble iodosylarenes, such as **1**, which, in combination with emerging MOF catalysts for C–H functionalization, would facilitate aerobic hydrocarbon oxidation chemistry.

Here, we show that a popular synthetic route to iodosylarene **1**, based on $KClO_3$ and HCl, affords material that displays unpredictable disproportionation rates. The un-

predictable behavior arises from trace impurities introduced during synthesis. We develop a new route, based on initial Cl_2 oxidation, that provides routine access to samples of **1** that display highly reproducible properties. Given the preparation-dependent disproportionation kinetics of **1**, in combination with differences in activity and solubility between iodosylarene **1** and iodylarene **2**, we believe that the results of catalytic reactions in which **1** is used as the terminal oxidant should be evaluated with care. We go on to investigate the coordination chemistry of $(PhIO)_n$ and iodosylarene **1** with soluble molecular transition metal clusters that resemble common components of MOF catalysts. We find that $(PhIO)_n$ participates in ligand exchange with both Zn_2- and Zr_6-based clusters to generate iodobenzene dicarboxylates. In contrast, iodosylarene **1** does not participate in exchange chemistry, but instead serves as a ligand to Zr_6 clusters. Examination of MOFs based on similar Zn_2 and Zr_6 sites indicates that the coordination chemistry of iodosylbenzenes with molecular clusters may be suppressed within materials, as the long-range structures of these materials are not perturbed upon exposure to iodosylbenzene derivatives. Given the interest in utilizing MOF catalysts in combination with hypervalent iodine-based oxidants for hydrocarbon upgrading, we anticipate that the observed coordination chemistry between transition metal clusters of iodosylbenzenes may be useful in designing robust catalyst materials.

ASSOCIATED CONTENT

Supporting Information

Detailed experimental procedures, spectral data, computational details, and coordinates of computed stationary points. Structures of **1**·HFIP and **7**·(**1**)$_4$ have been submitted to the CCDC as entries 1909655 and 1910636. This material is available free of charge via the Internet at http://pubs.acs.org.

AUTHOR INFORMATION

Corresponding Author

E-mail: david.powers@chem.tamu.edu

ORCID

A.M. 0000-0002-5923-8596
A.D.C. 0000-0002-0639-8596
W.-Y.G. 0000-0002-9879-1634
R.A. 0000-0002-0083-2275
S.-M.H. 0000-0001-6528-6685
D.C.P 0000-0003-3717-2001

Author Contributions

† These authors contributed equally to this work.

ACKNOWLEDGMENT

The authors acknowledge the National Science Foundation (CAREER 1848135) for supporting experiments in hypervalent iodine chemistry, the Department of Energy (DE-SC0018977) for supporting experiments in porous materials, and the Welch Foundation (A-1907) for financial support. The structure of **7**·(**1**)$_4$ was collected at the NSF's ChemMatCARS Sector 15, which is principally supported by the Divisions of Chemistry (CHE) and Materials Research (DMR), NSF, under grant number NSF/CHE-1346572. Use of the Advanced Photon Source, an Office of Science User Facility operated for the U.S. Department of Energy (DOE) Office of Science by Argonne National Laboratory, was supported by the U.S. DOE under Contract No. DE-AC02-06CH11357. Yu-Sheng Chen and Anuvab Das (X-ray diffraction) and Chen-Hao Wang (ICP-MS analysis) are thanked for experimental support.

REFERENCES

1. Greenwood, N. N.; Earnshaw, A. *Chemistry of the Elements*. Elsevier: 2012.
2. Pauling, L. *The Nature of the Chemical Bond*. Cornell University Press Ithaca, NY: 1960; Vol. 260.
3. Boschloo, G.; Hagfeldt, A. Characteristics of the Iodide/Triiodide Redox Mediator in Dye-Sensitized Solar Cells. *Acc. Chem. Res.* **2009**, *42*, 1819–1826.
4. Davies, C. G.; Gillespie, R. J.; Ireland, P. R.; Sowa, J. M. The Preparation and Crystal Structure of $[I_2]^+[Sb_2F_{11}]^-$. *Can. J. Chem.* **1974**, *52*, 2048–2052.
5. Kemmitt, R. D. W.; Murray, M.; McRae, V. M.; Peacock, R. D.; Symons, M. C. R.; Odonnell, R. A. The Iodine Cation, I^{2+}, in Antimony Pentafluoride. *J. Chem. Soc. A* **1968**, 862–866.
6. Faggiani, R.; Gillespie, R. J.; Kapoor, R.; Lock, C. J. L.; Vekris, J. E. Preparation and Solid-state and Solution Studies of Three Compounds of the Tetraiodine Dication I_4^{2+}: $I_4^{2+}(AsF_6^-)_2$, $I_4^{2+}(SbF_6^-)_2$, and $I_4^{2+}(Sb_3F_{14}^-)(SbF_6^-)$. *Inorg. Chem.* **1988**, *27*, 4350–4355.
7. Gillespie, R. J.; Kapoor, R.; Faggiani, R.; Lock, C. J. L.; Murchie, M.; Passmore, J. The I_4^{2+} cation. *X*-Ray crystal structures of $(I_4^{2+})(AsF_6^-)_2$ and $(I_4^{2+})(Sb_3F_{14}^-)(SbF_6^-)$. *J. Chem. Soc., Chem. Commun.* **1983**, 8–9.
8. Willgerodt, C. Ueber einige aromatische Jodidchloride. *J. Prakt. Chem.* **1886**, *33*, 154–160.
9. The oxidation state nomenclature is based on the ionic model and counting RIX_2 compounds as an iodine center with three X-type ligands.
10. Musher, J. I. The Chemistry of Hypervalent Molecules. *Angew. Chem. Int. Ed.* **1969**, *8*, 54–68.
11. Powell, W. H. Treatment of Variable Valence in Organic Nomenclature (Lambda-Convention). *Pure Appl. Chem.* **1984**, *56*, 769–778.
12. Martin, J. C. Frozen Transition-States - Pentavalent Carbon. *Science* **1983**, *221*, 509–514.
13. Perkins, C. W.; Martin, J. C.; Arduengo, A. J.; Lau, W.; Alegria, A.; Kochi, J. K. An Electrically Neutral σ-Sulfuranyl Radical from the Homolysis of a Perester with Neighboring Sulfenyl Sulfur: 9-S-3 Species. *J. Am. Chem. Soc.* **1980**, *102*, 7753–7759.
14. Zhdankin, V. V.; Stang, P. J. Recent Developments in the Chemistry of Polyvalent Iodine Compounds. *Chem. Rev.* **2002**, *102*, 2523–2584.
15. Stang, P. J.; Zhdankin, V. V. Organic Polyvalent Iodine Compounds. *Chem. Rev.* **1996**, *96*, 1123–1178.
16. Zhdankin, V. V. *Hypervalent Iodine Chemistry: Preparation, Structure and Synthetic Applications of Polyvalent Iodine Compounds*. John Wiley and Sons Ltd.: New York, 2014.
17. Zhdankin, V. V.; Stang, P. J. Chemistry of Polyvalent Iodine. *Chem. Rev.* **2008**, *108*, 5299–5358.
18. Yoshimura, A.; Zhdankin, V. V. Advances in Synthetic Applications of Hypervalent Iodine Compounds. *Chem. Rev.* **2016**, *116*, 3328–3435.
19. Ladziata, U.; Zhdankin, V. V. Hypervalent Iodine(V) Reagents in Organic Synthesis. *Arkivoc* **2006**, *9*, 26–58.
20. Reed, A. E.; Schleyer, P. v. R. Chemical Bonding in Hypervalent Molecules. The Dominance of Ionic Bonding and Negative Hyperconjugation over d-Orbital Participation. *J. Am. Chem. Soc.* **1990**, *112*, 1434–1445.
21. Hach, R. J.; Rundle, R. E. The Structure of Tetramethylammonium Pentaiodide. *J. Am. Chem. Soc.* **1951**, *73*, 4321–4324.
22. Pimentel, G. C. The Bonding of Trihalide and Bifluoride Ions by the Molecular Orbital Method. *J. Chem. Phys.* **1951**, *19*, 446–448.
23. Wang, W. Halogen Bond Involving Hypervalent Halogen: CSD Search and Theoretical Study. *J. Phys. Chem. A* **2011**, *115*, 9294–9299.
24. Cavallo, G.; Metrangolo, P.; Milani, R.; Pilati, T.; Priimagi, A.; Resnati, G.; Terraneo, G. The Halogen Bond. *Chem. Rev.* **2016**, *116*, 2478–2601.
25. Ochiai, M.; Sueda, T.; Miyamoto, K.; Kiprof, P.; Zhdankin, V. V. *trans* Influences on Hypervalent Bonding of Aryl λ^3-Iodanes: Their Stabilities and Isodesmic Reactions of Benziodoxolones and Benziodazolones. *Angew. Chem. Int. Ed.* **2006**, *45*, 8203–8206.
26. Ivanov, A. S.; Popov, I. A.; Boldyrev, A. I.; Zhdankin, V. V. The I=X (X=O, N, C) Double Bond in Hypervalent Iodine Compounds: Is it Real? *Angew. Chem. Int. Ed.* **2014**, *53*, 9617–9621.

27. Examples of monomeric iodosylbenzenes have been reported, see for examples: Hiller, A.; Pratt, J. T.; Steinbach, J. NMR study on the structure and stability of 4-substituted aromatic iodosyl compounds. *Magn. Reson. Chem.* **2006**, *44*, 955–958; Katritzky, A. R.; Gallos, J. K.; Durst, H. D. Structure of and Electronic Interactions in Aromatic Polyvalent Iodine Compounds: a ^{13}C NMR Study. *Magn. Reson. Chem.* **1989**, *27*, 815–822.
28. Carmalt, C. J.; Crossley, J. G.; Knight, J. G.; Lightfoot, P.; Martín, A.; Muldowney, M. P.; Norman, N. C.; Orpen, A. G. An Examination of the Structures of Iodosylbenzene (PhIO) and the Related Imido Compound, $PhINSO_2$-4-Me-C_6H_4, by X-Ray Powder Diffraction and EXAFS (Extended X-Ray Absorption Fine Structure) Spectroscopy. *J. Chem. Soc. Chem. Commun.* **1994**, 2367–2368.
29. Nemykin, V. N.; Koposov, A. Y.; Netzel, B. C.; Yusubov, M. S.; Zhdankin, V. V. Self-Assembly of Hydroxy(phenyl)iodonium Ions in Acidic Aqueous Solution: Preparation, and X-ray Crystal Structures of Oligomeric Phenyliodine(III) Sulfates. *Inorg. Chem.* **2009**, *48*, 4908–4917.
30. Protasiewicz, J. D. Organoiodine(III) Reagents as Active Participants and Ligands in Transition Metal-Catalyzed Reactions: Iodosylarenes and (Imino)iodoarenes. In *Hypervalent Iodine Chemistry*, Wirth, T., Ed. Springer International Publishing: Cham, 2016; pp 263–288.
31. Koposov, A. Y.; Karimov, R. R.; Pronin, A. A.; Skrupskaya, T.; Yusubov, M. S.; Zhdankin, V. V. $RuCl_3$-Catalyzed Oxidation of Iodoarenes with Peracetic Acid: New Facile Preparation of Iodylarenes. *J. Org. Chem.* **2006**, *71*, 9912–9914.
32. Lucas, H. J. K., E. R. Iodoxybenzene. *Org. Synth.* **1942**, *22*, 72.
33. Vasconcelos, R. S.; Silva, L. F.; Lopes, N. P. Study by Mass Spectrometry of Solutions of Hydroxy(Tosyloxy)Iodo Benzene: Proposed Disproportionation Mechanisms. *Quim. Nova* **2012**, *35*, 1593–1599.
34. Ochiai, M. *Reactivities, Properties and Structure*. Springer-Verlag: Berlin Heidelberg, 2003; Vol. 224.
35. Koser, G. F.; Wettach, R. H. Synthesis and Characterization of [Methoxy(tosyloxy)iodo]benzene, an Acyclic Monoalkoxyiodinane. *J. Org. Chem.* **1980**, *45*, 4988–4989.
36. Moriarty, R. M.; Prakash, O. Hypervalent Iodine in Organic Synthesis. *Acc. Chem. Res.* **1986**, *19*, 244–250.
37. McDonald, A. R.; Que, L., Jr. High-valent nonheme iron-oxo complexes: synthesis, structure, and spectroscopy. *Coord. Chem. Rev.* **2013**, *257*, 414–428.
38. Yamada, Y.; Kashima, K.; Okawara, M. Substituent Effect in the Nucleophilic Attack by the Bromide Ion on the *p*-Tolyl-Substituted Phenyliodonium Ions. *Bull. Chem. Soc. Japan* **1974**, *47*, 3179–3180.
39. England, J.; Guo, Y.; Farquhar, E. R.; Young, V. G., Jr.; Münck, E.; Que, L., Jr. The Crystal Structure of a High-Spin Oxoiron(IV) Complex and Characterization of Its Self-Decay Pathway. *J. Am. Chem. Soc.* **2010**, *132*, 8635–8644.
40. England, J.; Martinho, M.; Farquhar, E. R.; Frisch, J. R.; Bominaar, E. L.; Münck, E.; Que, L., Jr. A Synthetic High-Spin Oxoiron (IV) Complex: Generation, Spectroscopic Characterization, and Reactivity. *Angew. Chem. Int. Ed.* **2009**, *48*, 3622–3626.
41. White, M. C.; Zhao, J. Aliphatic C–H Oxidations for Late-Stage Functionalization. *J. Am. Chem. Soc.* **2018**, *140*, 13988–14009.
42. Kang, Y.; Li, X.-X.; Cho, K.-B.; Sun, W.; Xia, C.; Nam, W.; Wang, Y. Mutable Properties of Nonheme Iron(III)–Iodosylarene Complexes Result in the Elusive Multiple-Oxidant Mechanism. *J. Am. Chem. Soc.* **2017**, *139*, 7444–7447.
43. Singh, F. V.; Wirth, T. Hypervalent Iodine-Catalyzed Oxidative Functionalizations Including Stereoselective Reactions. *Chem. Asian J.* **2014**, *9*, 950–971.
44. Yusubov, M. S. Y., A. Zhdankin, V. V. Iodonium ylides in organic synthesis. *Arkivoc* **2016**, 342–364.
45. Zhdankin, V. V.; Stang, P. J. Chemistry of Polyvalent Iodine. *Chem. Rev.* **2008**, *108*, 5299–5358.
46. Dunn, N. L.; Ha, M.; Radosevich, A. T. Main Group Redox Catalysis: Reversible P^{III}/P^{V} Redox Cycling at a Phosphorus Platform. *J. Am. Chem. Soc.* **2012**, *134*, 11330–11333.
47. Hilton, M. C.; Zhang, X.; Boyle, B. T.; Alegre-Requena, J. V.; Paton, R. S.; McNally, A. Heterobiaryl synthesis by contractive C–C coupling via P(V) intermediates. *Science* **2018**, *362*, 799–804.
48. Nykaza, T. V.; Cooper, J. C.; Li, G.; Mahieu, N.; Ramirez, A.; Luzung, M. R.; Radosevich, A. T. Intermolecular Reductive C–N Cross Coupling of Nitroarenes and Boronic Acids by P^{III}/P^{V}=O Catalysis. *J. Am. Chem. Soc.* **2018**, *140*, 15200–15205.
49. Nykaza, T. V.; Harrison, T. S.; Ghosh, A.; Putnik, R. A.; Radosevich, A. T., A Biphilic Phosphetane Catalyzes N–N Bond-Forming Cadogan Heterocyclization via P^{III}/P^{V}=O Redox Cycling. *J. Am. Chem. Soc.* **2017**, *139*, 6839–6842.
50. Moriarty, R. M.; Prakash, O. Oxidation of Carbonyl Compounds with Organohypervalent Iodine Reagents. *Org. React.* **1999**, 54, 273–418.
51. Nicolaou, K. C.; Simmons, N. L.; Ying, Y.; Heretsch, P. M.; Chen, J. S. Enantioselective Dichlorination of Allylic Alcohols. *J. Am. Chem. Soc.* **2011**, *133*, 8134–8137.
52. Turner, C. D.; Ciufolini, M. A. Oxidation of oximes with hypervalent iodine reagents: opportunities, development, and applications. *Arkivoc* **2011**, 410–428.
53. Ciufolini, M. A. B.; Norbert A.; Canesi, S.; Ousmer, M.; Chang, J.; Chai, D. Oxidative Amidation of Phenols through the Use of Hypervalent Iodine Reagents: Development and Applications. *Synthesis* **2007**, 3759–3772.
54. Moriarty, R. M.; Prakash, O. Oxidation of Phenolic Compounds with Organohypervalent Iodine Reagents. *Org. React.* **2001**, *57*, 327–415.
55. Pouységu, L.; Deffieux, D.; Quideau, S. Hypervalent iodine-mediated phenol dearomatization in natural product synthesis. *Tetrahedron* **2010**, *66*, 2235–2261.
56. Samanta, R.; Matcha, K.; Antonchick, A. P. Metal-Free Oxidative Carbon-Heteroatom Bond Formation Through C–H Bond Functionalization. *Eur. J. Org. Chem.* **2013**, 5769–5804.
57. Moreno, I.; Tellitu, I.; Herrero, M. T.; SanMartin, R.; Dominguez, E. New Perspectives for Iodine(III) Reagents in (Hetero)Biaryl Coupling Reactions. *Curr. Org. Chem.* **2002**, *6*, 1433–1452.
58. Charpentier, J.; Fruh, N.; Togni, A. Electrophilic Trifluoromethylation by Use of Hypervalent Iodine Reagents. *Chem. Rev.* **2014**, *115*, 650–682.
59. Gao, W.-Y.; Cardenal, A. D.; Wang, C.-H.; Powers, D. C. In Operando Analysis of Diffusion in Porous Metal-Organic Framework Catalysts. *Chem. Eur. J.* **2019**, *25*, 3465–3476.
60. Xiao, D. J.; Oktawiec, J.; Milner, P. J.; Long, J. R. Pore Environment Effects on Catalytic Cyclohexane Oxidation in Expanded Fe_2(dobdc) Analogues. *J. Am. Chem. Soc.* **2016**, *138*, 14371–14379.
61. Stubbs, A. W.; Braglia, L.; Borfecchia, E.; Meyer, R. J.; Román-Leshkov, Y.; Lamberti, C.; Dincă, M. Selective Catalytic Olefin Epoxidation with Mn^{II}-Exchanged MOF-5. *ACS Catal.* **2018**, *8*, 596–601.
62. Song, F.; Wang, C.; Falkowski, J. M.; Ma, L.; Lin, W. Isoreticular Chiral Metal−Organic Frameworks for Asymmetric Alkene Epoxidation: Tuning Catalytic Activity by Controlling Framework Catenation and Varying Open Channel Sizes. *J. Am. Chem. Soc.* **2010**, *132*, 15390–15398.
63. Wang, L.; Agnew, D. W.; Yu, X.; Figueroa, J. S.; Cohen, S. M. A Metal–Organic Framework with Exceptional Activity for C−H Bond Amination. *Angew. Chem. Int. Ed.* **2018**, *57*, 511–515.
64. Xia, Q.; Li, Z.; Tan, C.; Liu, Y.; Gong, W.; Cui, Y. Multivariate Metal–Organic Frameworks as Multifunctional Heterogeneous Asymmetric Catalysts for Sequential Reactions. *J. Am. Chem. Soc.* **2017**, *139*, 8259–8266.
65. The secondary bonding interactions that are responsible for the availability of monomeric iodosylarene **1** could also be described as interactions of the pendent sulfonylgroup with the sigma-hole of the I–O bond. See, Politzer, P.; Murray, J. S.; Clark, T. Halogen bonding and other σ-hole interactions: a perspective. *Phys. Chem. Chem. Phys.* **2013**, 15, 11178–11189.
66. Maity, A.; Hyun, S. M.; Powers, D. C. Oxidase Catalysis via Aerobically Generated Hypervalent Iodine Intermediates. *Nat. Chem.* **2018**, *10*, 200–204.
67. Macikenas, D.; Skrzypczak-Jankun, E.; Protasiewicz, J. D. A New Class of Iodonium Ylides Engineered as Soluble Primary Oxo and Nitrene Sources. *J. Am. Chem. Soc.* **1999**, *121*, 7164–7165.
68. Sajith, P. K.; Suresh, C. H. Quantification of the Trans Influence in Hypervalent Iodine Complexes. *Inorg. Chem.* **2012**, *51*, 967–977.
69. Kita, Y.; Tohma, H.; Inagaki, M.; Hatanaka, K.; Yakura, T. A novel oxidative azidation of aromatic compounds with hypervalent iodine reagent, phenyliodine(III) bis(trifluoroacetate) (PIFA) and trimethylsilyl azide. *Tetrahedron Lett.* **1991**, *32*, 4321–4324.
70. Kita, Y.; Tohma, H.; Hatanaka, K.; Takada, T.; Fujita, S.; Mitoh, S.; Sakurai, H.; Oka, S. Hypervalent Iodine-Induced Nucleophilic Substitution of *para*-Substituted Phenol Ethers. Generation of Cation Radicals as Reactive Intermediates. *J. Am. Chem. Soc.* **1994**, *116*, 3684–3691.
71. Hamamoto, H.; Hata, K.; Nambu, H.; Shiozaki, Y.; Tohma, H.; Kita, Y. A novel and direct synthesis of chroman derivatives using a hypervalent iodine(III) reagent. *Tetrahedron Lett.* **2004**, *45*, 2293–2295.
72. Kita, Y.; Morimoto, K.; Ito, M.; Ogawa, C.; Goto, A.; Dohi, T. Metal-Free Oxidative Cross-Coupling of Unfunctionalized Aromatic Compounds. *J. Am. Chem. Soc.* **2009**, *131*, 1668–1669.

73. Dohi, T.; Ito, M.; Yamaoka, N.; Morimoto, K.; Fujioka, H.; Kita, Y. Unusual *ipso* Substitution of Diaryliodonium Bromides Initiated by a Single-Electron-Transfer Oxidizing Process. *Angew. Chem. Int. Ed.* **2010**, *49*, 3334–3337.

74. Ito, M.; Kubo, H.; Itani, I.; Morimoto, K.; Dohi, T.; Kita, Y. Organocatalytic C–H/C–H′ Cross-Biaryl Coupling: C-Selective Arylation of Sulfonanilides with Aromatic Hydrocarbons. *J. Am. Chem. Soc.* **2013**, *135*, 14078–14081.

75. Macikenas, D.; Skrzypczak-Jankun, E.; Protasiewicz, J. D. Redirecting Secondary Bonds to Control Molecular and Crystal Properties of an Iodosyl- and an Iodylbenzene. *Angew. Chem. Int. Ed.* **2000**, *39*, 2007–2010.

76. Schardt, B. C.; Hill, C. L. Preparation of Iodobenzene Dimethoxide. A New Synthesis of [^{18}O]Iodosylbenzene and a Reexamination of Its Infrared Spectrum. *Inorg. Chem.* **1983**, *22*, 1563–1565.

77. Kajiyama, D.; Saitoh, T.; Nishiyama, S. Application of Electrochemically Generated Hypervalent Iodine Oxidant to Natural Products Synthesis. *Electrochemistry* **2013**, *81*, 319–324.

78. Broese, T.; Francke, R. Electrosynthesis Using a Recyclable Mediator–Electrolyte System Based on Ionically Tagged Phenyl Iodide and 1,1,1,3,3,3-Hexafluoroisopropanol. *Org. Lett.* **2016**, *18*, 5896–5899.

79. Koleda, O.; Broese, T.; Noetzel, J.; Roemelt, M.; Suna, E.; Francke, R. Synthesis of Benzoxazoles Using Electrochemically Generated Hypervalent Iodine. *J. Org. Chem.* **2017**, *82*, 11669–11681.

80. Maity, A.; Hyun, S.-M.; Wortman, A. K.; Powers, D. C. Oxidation Catalysis by an Aerobically Generated Dess–Martin Periodinane Analogue. *Angew. Chem. Int. Ed.* **2018**, *57*, 7205–7209.

81. Richter, H. W.; Cherry, B. R.; Zook, T. D.; Koser, G. F. Characterization of Species Present in Aqueous Solutions of [Hydroxy(mesyloxy)iodo]benzene and [Hydroxy(tosyloxy)iodo]benzene. *J. Am. Chem. Soc.* **1997**, *119*, 9614–9623.

82. Silva, L. F., Jr.; Vasconcelos, R. S.; Lopes, N. P. Application of high-resolution electrospray mass spectrometry for the elucidation of the disproportionation reaction of iodobenzene diacetate. *Int. J. Mass Spectrom.* **2008**, *276*, 24–30.

83. Macikenas, D.; Skrzypczak-Jankun, E.; Protasiewicz, J. D. A New Class of Iodonium Ylides Engineered as Soluble Primary Oxo and Nitrene Sources. *J. Am. Chem. Soc.* **2011**, *133*, 4151–4151.

84. Guo, M.; Dong, H.; Li, J.; Cheng, B.; Huang, Y.-Q.; Feng, Y.-Q.; Lei, A. Spectroscopic observation of iodosylarene metalloporphyrin adducts and manganese(V)-oxo porphyrin species in a cytochrome P450 analogue. *Nat. Commun.* **2012**, *3*, 1190.

85. Sankar, M.; Nowicka, E.; Carter, E.; Murphy, D. M.; Knight, D. W.; Bethell, D.; Hutchings, G. J. The benzaldehyde oxidation paradox explained by the interception of peroxy radical by benzyl alcohol. *Nat. Commun.* **2014**, *5*, 3332.

86. Domae, M.; Katsumara, Y.; Jiang, P. Y.; Nagaishi, R.; Hasegawa, C.; Ishigure, K.; Yoshida, Y. Observation of Chlorine Oxide (ClO_3) Radical in Aqueous Chlorate Solution by Pulse Radiolysis. *J. Phys. Chem.* **1994**, *98*, 190–192.

87. Çatir, M.; Kilic, H.; Nardello-Rataj, V.; Aubry, J.-M.; Kazaz, C. Singlet Oxygen Generation from [Bis(trifluoroacetoxy)iodo]benzene and Hydrogen Peroxide. *J. Org.Chem.* **2009**, *74*, 4560–4564.

88. Çatir, M. Singlet oxygen generation from poly[4-diacetoxyiodo]styrene and hydrogen peroxide. *Turk. J. Chem.* **2017**, *41*, 467–475.

89. Tahmouresilerd, B.; Moody, M.; Agogo, L.; Cozzolino, A. F. The impact of an isoreticular expansion strategy on the performance of iodine catalysts supported in multivariate zirconium and aluminum metal–organic frameworks. *Dalton Trans.* **2019**, *48*, 6445–6454.

90. Shultz, A. M.; Farha, O. K.; Adhikari, D.; Sarjeant, A. A.; Hupp, J. T.; Nguyen, S. T. Selective Surface and Near-Surface Modification of a Noncatenated, Catalytically Active Metal-Organic Framework Material Based on Mn(salen) Struts. *Inorg. Chem.* **2011**, *50*, 3174–3176.

91. Dey, D.; Roy, S.; Dutta Purkayastha, R. N.; Pallepogu, R.; Male, L.; McKee, V. Syntheses, characterization, and crystal structures of two zinc(II) carboxylates containing pyridine. *J. Coord. Chem.* **2011**, *64*, 1165–1176.

92. Kickelbick, G.; Schubert, U. Oxozirconium Methacrylate Clusters: $Zr_6(OH)_4O_4(OMc)_{12}$ and $Zr_4O_2(OMc)_{12}$ (OMc = Methacrylate). *Chem. Ber.* **1997**, *130*, 473–478.

93. Kogler, F. R.; Jupa, M.; Puchberger, M.; Schubert, U. Control of the ratio of functional and non-functional ligands in clusters of the type $Zr_6O_4(OH)_4(carboxylate)_{12}$ for their use as building blocks for inorganic–organic hybrid polymers. *J. Mater. Chem.* **2004**, *14*, 3133–3138.

94. Kalmutzki, M. J.; Hanikel, N.; Yaghi, O. M. Secondary building units as the turning point in the development of the reticular chemistry of MOFs. *Sci. Adv.* **2018**, *4*, eaat9180.

95. Yuan, S.; Qin, J.-S.; Lollar, C. T.; Zhou, H.-C. Stable Metal–Organic Frameworks with Group 4 Metals: Current Status and Trends. *ACS Cent. Sci.* **2018**, *4*, 440–450.

96. Turlington, C. R.; Morris, J.; White, P. S.; Brennessel, W. W.; Jones, W. D.; Brookhart, M.; Templeton, J. L. Exploring Oxidation of Half-Sandwich Rhodium Complexes: Oxygen Atom Insertion into the Rhodium–Carbon Bond of κ2-Coordinated 2-Phenylpyridine. *Organometallics* **2014**, *33*, 4442–4448.

97. Lennartson, A.; McKenzie, C. J. An Iron(III) Iodosylbenzene Complex: A Masked Non-Heme $Fe^{V}O$. *Angew. Chem. Int. Ed.* **2012**, *51*, 6767–6770.

98. Wang, C.; Kurahashi, T.; Fujii, H. Structure and Reactivity of an Iodosylarene Adduct of a Manganese(IV)–Salen Complex. *Angew. Chem. Int. Ed.* **2012**, *51*, 7809–7811.

99. Hill, E. A.; Kelty, M. L.; Filatov, A. S.; Anderson, J. S. Isolable Iodosylarene and Iodoxyarene Adducts of Co and Their O-atom Transfer and C–H Activation Reactivity. *Chem. Sci.* **2018**, *9*, 4493–4499.

100. de Ruiter, G.; Carsch, K. M.; Gul, S.; Chatterjee, R.; Thompson, N. B.; Takase, M. K.; Yano, J.; Agapie, T. Accelerated Oxygen Atom Transfer and C−H Bond Oxygenation by Remote Redox Changes in Fe_3Mn-Iodosobenzene Adducts. *Angew. Chem. Int. Ed.* **2017**, *56*, 4772–4776.

101. Cavka, J. H.; Jakobsen, S.; Olsbye, U.; Guillou, N.; Lamberti, C.; Bordiga, S.; Lillerud, K. P. A New Zirconium Inorganic Building Brick Forming Metal Organic Frameworks with Exceptional Stability. *J. Am. Chem. Soc.* **2008**, *130*, 13850–13851.

102. Chen, B.; Liang, C.; Yang, J.; Contreras, D. S.; Clancy, Y. L.; Lobkovsky, E. B.; Yaghi, O. M.; Dai, S. A Microporous Metal–Organic Framework for Gas-Chromatographic Separation of Alkanes. *Angew. Chem. Int. Ed.* **2006**, *45*, 1390–1393.

103. MOF-508 features a nominal pore size of 4.0 × 4.0 Å and compound **1** has an approximate van der Waals diameter of 7.6 Å, suggesting that it is too large to enter the pores of MOF-508. However, MOF-508 displays network flexibility and has been demonstrated to uptake guests larger than the nominal pore size (*i.e* 2,2-dimethylbutane, van der Waals diameter of 6.3 Å. Goblin, O. C.; Reitmeier, S. J.; Jentys, A.; Lercher, J. A. *J. Phys. Chem. C* **2011**, *115*, 1171–1179).

104. Han, D.; Jiang, F. L.; Wu, M. Y.; Chen, L.; Chen, Q. H.; Hong, M. C. A non-interpenetrated porous metal-organic framework with high gas-uptake capacity. *Chem. Commun.* **2011**, *47*, 9861–9863.

105. Klein, N.; Senkovska, I.; Baburin, I. A.; Grunker, R.; Stoeck, U.; Schlichtenmayer, M.; Streppel, B.; Mueller, U.; Leoni, S.; Hirscher, M.; Kaskel, S. Route to a Family of Robust, Non-interpenetrated Metal-Organic Frameworks with pto-like Topology. *Chem. Eur. J.* **2011**, *17*, 13007–13016.

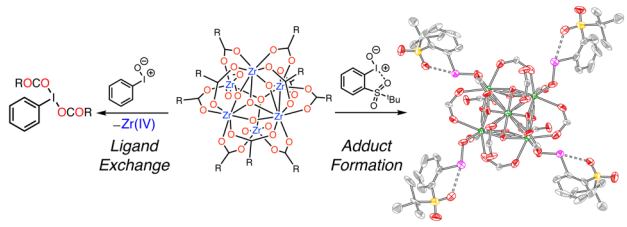
ROCO
OCOR
–Zr(IV)
Ligand
Exchange
Adduct
Formation